PROCEEDINGS OF SCIENCE

# Elimination of QCD Renormalization Scale and Scheme Ambiguities

**Leonardo Di Giustino**,[a,b,*] **Stanley J. Brodsky** ,[c] **Philip G. Ratcliffe**,[a,b] **Xing-Gang Wu**[d] **and Sheng-Quan Wang**[e]

[a] *Department of Science and High Technology, University of Insubria, via Valleggio 11, I-22100, Como, Italy*

[b] *INFN, Sezione di Milano–Bicocca, 20126 Milano, Italy*

[c] *SLAC National Accelerator Laboratory, Stanford University, Stanford, California 94039, USA*

[d] *Department of Physics, Chongqing University, Chongqing 401331, P.R. China*

[e] *Department of Physics, Guizhou Minzu University, Guiyang 550025, P.R. China*

*E-mail:* leonardo.digiustino@uninsubria.it, sjbth@slac.stanford.edu, philip.ratcliffe@uninsubria.it, wuxg@cqu.edu.cn, sqwang@alu.cqu.edu.cn

We present results for the thrust distribution in the electron positron annihilation to the three jet process at NNLO in the perturbative conformal window of QCD, as a function of the number of flavors $N_f$. Given the existence of an infrared interacting fixed point in this region, we can compare the Conventional Scale Setting (CSS) and the Principle of Maximum Conformality ($\text{PMC}_\infty$) methods along the entire renormalization group flow from the highest energies to zero energy. We then consider also the QED thrust, obtained as the limit $N_c \to 0$ of the number of colors and we show analogous comparison. QED in the low energy regime develops an infrared non-interacting fixed point. Using these quantum field theory limits as theoretical laboratories, we arrive at interesting results showing new features of the $\text{PMC}_\infty$.

*16th International Symposium on Radiative Corrections: Applications of Quantum Field Theory to Phenomenology ( RADCOR2023)*
*28th May - 2nd June, 2023*
*Crieff, Scotland, UK*

*Speaker





PoS(RADCOR2023)071

## 1. Introduction

The renormalization scale and scheme ambiguities are important sources of errors, which greatly affect the results of the Conventional Scale Setting (CSS) in perturbative QCD calculations. Given the high precision reached by the experiments at LEP and SLAC [1–5] in the measurement of the event shape variables and accuracy achieved by higher order calculations from next-to-leading order (NLO) calculations [6–11] to the next-to-next-to-leading order(NNLO) [12–16] and including resummation of the large logarithms [17, 18], the elimination of the uncertainties related to the scheme and scale ambiguities is crucial in order to improve the results and to test the Standard Model to the highest possible precision. In the particular case of the three-jet event-shape distributions the conventional practice of CSS leads to results which are in conflict with experimental data and the extracted values of $\alpha_s$ deviate from the world average [19]. A solution to the renormalization scale ambiguity problem is provided by the *Principle of Maximum Conformality* (PMC) [20–28]. This method provides a systematic way to eliminate renormalization scheme-and-scale ambiguities from first principles by absorbing the $\beta$ terms that govern the behavior of the running coupling via the renormalization group equation. This procedure is scheme-independent and leads to results free from divergent renormalon terms [29]. The PMC procedure is consistent with the standard Gell-Mann–Low method in the Abelian limit, $N_c \to 0$ [30] and can be considered the non-Abelian extension of the Serber–Uehling [31, 32] scale setting, which is essential for precision tests of QED and atomic physics. It should be emphasized that in a theory of unification of all forces, electromagnetic, weak and strong interactions, such as the Standard Model, or Grand Unification theories, one cannot simply apply a different scale-setting or analytic procedure to different sectors of the theory. The PMC offers the possibility to apply the same method in all sectors of a theory, starting from first principles, eliminating the renormalon growth, the scheme dependence, scale ambiguities while satisfying the QED Gell-Mann-Low scale-setting in the zero-color limit $N_c \to 0$. We remark that PMC leads to scheme invariant results.

We refer to RS-scheme invariance as the invariance under the extended-renormalization group and its equations (xRGE)[1]. Any other relation among different quantities defined in different approximations or obtained using different approaches, that can have perturbative validity in QCD, can be improved using the PMC and the residual dependence on the particular definition of the "scheme" can be suppressed perturbatively by adding higher order calculations. It can be shown that also in this case the results obtained are scheme-independent (see Ref. [37]). We remark that in order to apply the PMC correctly, one should be able to distinguish among the nature of the different $n_f$-terms, whether they are

[1] A recent argument on PMC by Stevenson [33], based on the principle of minimum sensitivity (PMS), is incorrect. Since the PMS is based on the assumption that all the unknown higher-order terms give zero contribution to the pQCD series [34], its prediction directly breaks the standard renormalization group invariance [26, 27], its pQCD series does not have normal perturbative features [35] and can be treated as an effective prediction only when we know the series up to high enough orders and the conventional series has already shown good perturbative features [36]. On the other hand, the PMC respects all features of the renormalization group, and its prediction satisfies all the requirements of standard renormalization group invariance [26, 27, 37, 38]. A detailed discussion on this point will be presented soon.

related to the running of the coupling, to the running of masses or to UV-finite diagrams and in a deeper analysis also to the particular UV-divergent diagram (as discussed in Refs. [39, 40]). Once all $n_f$-terms have been associated with the correct diagram or parameter, conformal coefficients are RG invariant and match the coefficients of a conformal theory. Moreover, given that the PMC preserves the RG invariance, it is possible to define CSR - Commensurate Scale Relations[25] among the effective charges relating observables in different "schemes" preserving all the group properties. Applying the PMC and the CSRs, one can relate effective couplings, as also conformal coefficients, leading to scheme independent results for the observables. Applications of the PMC to different quantities (see Ref. [41, 42]) have recently shown a direct improvement of theoretical predictions.

The recently developed *Infinite-Order Scale-Setting using the Principle of Maximum Conformality* ($\text{PMC}_\infty$) has been shown to significantly reduce the theoretical errors in Event Shape Variable distributions, highly improving also the fit with the experimental data[39, 43–45]. An improved theoretical prediction on $\alpha_s$ with respect to the world average has also been shown in Refs.[46, 47]. In this article we consider the thrust distribution in the region of flavors and colors near the upper bound of the conformal window, i.e. $N_f \sim 11/2N_c$ , where the IR fixed point can be reliably accessed in perturbation theory and we compare the two renormalization scale setting methods, the CSS and the $\text{PMC}_\infty$. In this region we are able to deduce the full solution at NNLO in the strong coupling. We also compare the two methods in the QED, $N_c \to 0$, limit of thrust.

## 2. Two-loop solution and the perturbative conformal window

The strong coupling dependence on the scale can be described introducing the $\beta$-function given by:

$$\frac{1}{4\pi}\frac{d\alpha_s(Q^2)}{d\log Q^2} = \beta(\alpha_s), \tag{1}$$

and

$$\beta\left(\alpha_s\right) = -\left(\frac{\alpha_s}{4\pi}\right)^2 \sum_{n=0}\left(\frac{\alpha_s}{4\pi}\right)^n \beta_n. \tag{2}$$

Neglecting quark masses, the first two $\beta$-terms are RS independent and they have been calculated in Refs. [48–52]:

$$\beta_0 = \frac{11}{3}C_A - \frac{4}{3}T_R N_f, \tag{3}$$

$$\beta_1 = \frac{34}{3}C_A^2 - 4\left(\frac{5}{3}C_A + C_F\right)T_R N_f, \tag{4}$$

where $C_F = \frac{\left(N_c^2-1\right)}{2N_c}$, $C_A = N_c$ and $T_R = 1/2$ are the color factors for the SU(3) gauge group [53].

In order to determine the solution for the strong coupling $\alpha_s$ at NNLO, it is convenient to introduce the following notation: $x(\mu) \equiv \frac{\alpha_s(\mu)}{2\pi}$, $t = \log(\mu^2/\mu_0^2)$, $B = \frac{1}{2}\beta_0$ and $C = \frac{1}{2}\frac{\beta_1}{\beta_0}$, $x^* \equiv -\frac{1}{C}$. The truncated NNLO approximation of the Eq. 1 leads to the differential

equation:

$$\frac{dx}{dt} = -Bx^2(1+Cx). \tag{5}$$

An implicit solution of Eq. 5 is given by the Lambert $W(z)$ function:

$$We^W = z, \tag{6}$$

with: $W = \left(\frac{x^*}{x} - 1\right)$. The general solution for the coupling is:

$$x = \frac{x^*}{1+W}, \tag{7}$$

$$z = e^{\frac{x^*}{x_0}-1}\left(\frac{x^*}{x_0}-1\right)\left(\frac{\mu^2}{\mu_0^2}\right)^{x^*B}. \tag{8}$$

We shall discuss here the solutions to Eq. 5 with respect to the particular initial phenomenological value $x_0 \equiv \alpha_s(M_Z)/(2\pi) = 0.01876 \pm 0.00016$ given by the coupling determined at the $Z^0$ mass scale [19]. This value introduces an upper boundary on the number of flavors: $\bar{N}_f = x^{*-1}(x_0) = 15.222 \pm 0.009$, which narrows the range for the IR fixed point discussed by Banks and Zaks [54]. The only physically accessible range is $N_f < \bar{N}_f$, since for $N_f > \bar{N}_f$ we no longer have the asymptotically free UV behavior. In the range $N_f < \bar{N}_f^1$ we have $B > 0$, $C > 0$ and the physical solution is given by the $W_{-1}$ branch (i.e. the solution of Eq. 6 with $-\frac{1}{e} < z < 0$ and $W < -1$), while for $\bar{N}_f^1 < N_f < \bar{N}_f$ the solution for the strong coupling is given by the $W_0$ branch (i.e. the solution of Eq. 6 with $z > 0$ and $W > 0$); a detailed description of the Lambert solutions is given in Ref. [55]. Where the values $\bar{N}_f^0 = \frac{11}{2}N_c$, $\bar{N}_f^1 = \frac{34N_c^3}{13N_c^2-3}$, with $\bar{N}_f^0 > \bar{N}_f^1$, are the zeros of $\beta_0, \beta_1$ respectively. The two-dimensional region in the number of flavors and colors where asymptotically free QCD develops an IR interacting fixed point is colloquially known as the *conformal window of pQCD*. In general, IR and UV fixed points of the $\beta$-function can also be determined at different values of the number of colors $N_c$ (different gauge group $SU(N)$) and $N_f$ extending this analysis also to other gauge theories [56]. An extension of the perturbative QCD coupling and its $\beta$-function in the IR region can be found in Ref. [57].

## 3. The thrust distribution according to $N_f$

The thrust distribution and the event shape variables are a fundamental tool in order to probe the geometrical structure of a given process at colliders and for the measurement of the strong coupling $\alpha_s$ [58]. Thrust ($T$) is defined as

$$T = \max_{\vec{n}}\left(\frac{\sum_i |\vec{p}_i \cdot \vec{n}|}{\sum_i |\vec{p}_i|}\right), \tag{9}$$

where the sum runs over all particles in the hadronic final state, and $\vec{p}_i$ denotes the three-momentum of particle $i$. The unit vector $\vec{n}$ is varied to maximize thrust $T$, and the corresponding $\vec{n}$ is called the thrust axis and denoted by $\vec{n}_T$. The variable $(1-T)$ is often used, which for the LO of 3-jet production is restricted to the range $(0 < 1-T < 1/3)$. We

have a back-to-back or a spherically symmetric event respectively at $T = 1$ and at $T = 2/3$ respectively.

In general, a normalized IR-safe single-variable observable, such as the thrust distribution for the $e^+e^- \to 3jets$ [59, 60], is the sum of pQCD contributions calculated up to NNLO at the initial renormalization scale $\mu_0 = \sqrt{s} = M_Z$:

$$\frac{1}{\sigma_{tot}}\frac{Od\sigma(\mu_0)}{dO} = \left\{x_0 \cdot \frac{Od\overline{A}_O(\mu_0)}{dO} + x_0^2 \cdot \frac{Od\overline{B}_O(\mu_0)}{dO} + x_0^3 \cdot \frac{Od\overline{C}_O(\mu_0)}{dO} + \mathcal{O}(\alpha_s^4)\right\} \tag{10}$$

where $x(\mu) \equiv \alpha_s(\mu)/(2\pi)$, $O$ is the selected event shape variable, $\sigma$ the cross section of the process,

$$\sigma_{tot} = \sigma_0\left(1 + x_0 A_{tot} + x_0^2 B_{tot} + \mathcal{O}\left(\alpha_s^3\right)\right), \tag{11}$$

is the total hadronic cross section and $\overline{A}_O, \overline{B}_O, \overline{C}_O$ are respectively the normalized LO, NLO and NNLO coefficients:

$$\begin{aligned} \overline{A}_O &= A_O, \\ \overline{B}_O &= B_O - A_{tot}A_O, \\ \overline{C}_O &= C_O - A_{tot}B_O - \left(B_{tot} - A_{tot}^2\right)A_O, \end{aligned} \tag{12}$$

where $A_O, B_O, C_O$ are the coefficients normalized to the tree-level cross section $\sigma_0$ calculated by MonteCarlo (see e.g. the EERAD and Event2 codes [12–16]) and $A_{tot}, B_{tot}$ are:

$$\begin{aligned} A_{tot} &= \frac{3}{2}C_F, \\ B_{tot} &= \frac{C_F}{4}N_c + \frac{3}{4}C_F\frac{\beta_0}{2}(11 - 8\zeta(3)) - \frac{3}{8}C_F^2, \end{aligned} \tag{13}$$

where $\zeta$ is the Riemann zeta function. In the case of conventional scale setting, the renormalization scale is set to $\mu_0 = \sqrt{s} = M_Z$ and theoretical uncertainties are evaluated using standard criteria. In this case, we have used the definition given in Ref. [13] of the parameter $\delta$; we define the average error for the event shape variable distributions as:

$$\bar{\delta} = \frac{1}{N}\sum_i^N \frac{\max_\mu(\sigma_i(\mu)) - \min_\mu(\sigma_i(\mu))}{2\sigma_i(\mu = M_Z)}, \tag{14}$$

where $i$ is the index of the bin and $N$ is the total number of bins, the renormalization scale is varied in the range: $\mu \in [M_Z/2; 2M_Z]$. We use here the two-loop solution for the running coupling $\alpha_s(Q)$. According to the PMC$_\infty$ (for a detailed analysis see Ref. [39, 44, 45]), Eq. 10 becomes:

$$\frac{1}{\sigma_{tot}}\frac{Od\sigma(\mu_{\rm I}, \tilde{\mu}_{\rm II}, \mu_0)}{dO} = \left\{\overline{\sigma}_{\rm I} + \overline{\sigma}_{\rm II} + \overline{\sigma}_{\rm III} + \mathcal{O}(\alpha_s^4)\right\}, \tag{15}$$

where the $\overline{\sigma}_N$ are normalized subsets given by:

$$\begin{aligned}
\overline{\sigma}_{\rm I} &= A_{Conf}\cdot x_{\rm I},\\
\overline{\sigma}_{\rm II} &= (B_{Conf}+\eta A_{tot}A_{Conf})\cdot x_{\rm II}^2-\eta A_{\rm tot}A_{Conf}\cdot x_0^2\\
&\qquad -A_{\rm tot}A_{Conf}\cdot x_0 x_{\rm I},\\
\overline{\sigma}_{\rm III} &= \left(C_{Conf}-A_{\rm tot}B_{Conf}-(B_{\rm tot}-A_{\rm tot}^2)A_{Conf}\right)\cdot x_0^3,
\end{aligned}\tag{16}$$

where $A_{Conf}, B_{Conf}, C_{Conf}$ are the scale-invariant conformal coefficients (i.e. the coefficients of each perturbative order not depending on the scale $\mu_R$) while $x_{\rm I}, x_{\rm II}, x_0$ are the couplings determined at the PMC$_\infty$ scales: $\mu_{\rm I}, \tilde{\mu}_{\rm II}, M_Z$ respectively. The PMC$_\infty$ scales are given by:

$$\mu_{\rm I} = \sqrt{s}\cdot e^{f_{sc}-\frac{1}{2}B_{\beta_0}} \qquad (1-T)<0.33, \tag{17}$$

$$\tilde{\mu}_{\rm II} = \begin{cases} \sqrt{s}\cdot e^{f_{sc}-\frac{1}{2}C_{\beta_0}\cdot\frac{B_{Conf}}{B_{Conf}+\eta\cdot A_{tot}A_{Conf}}} & (1-T)<0.33,\\ \sqrt{s}\cdot e^{f_{sc}-\frac{1}{2}C_{\beta_0}}, & (1-T)>0.33, \end{cases} \tag{18}$$

where the $f_{sc}$ is a general scheme factor which is $f_{sc}\equiv 0$ for the QCD case in $\overline{\rm MS}$-scheme. Normalized subsets for the region $(1-T)>0.33$ can be simply achieved by setting $A_{Conf}\equiv 0$ in the Eq. 16. Results for the thrust distribution calculated using the NNLO solution for the coupling $\alpha_s(\mu)$, at different values of the number of flavors, $N_f$, is shown in Fig. 1.

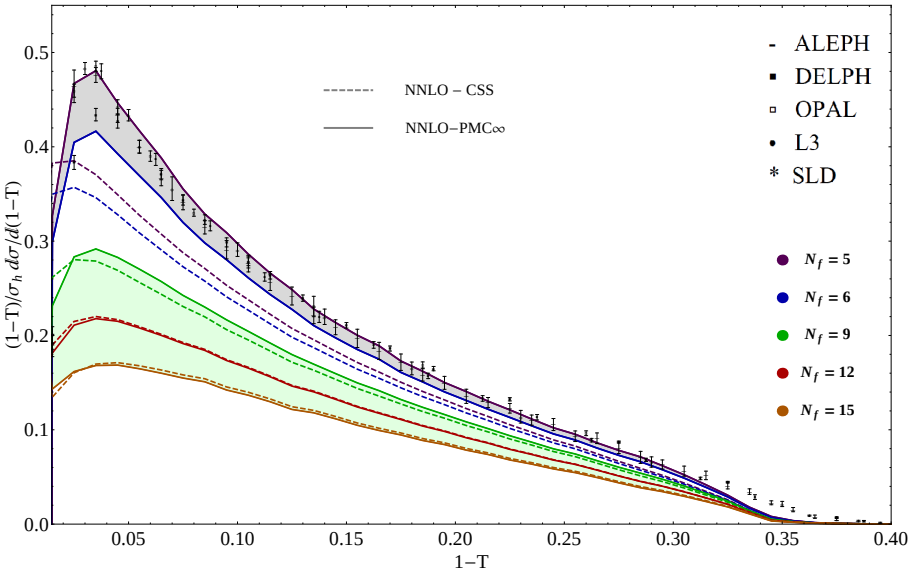


**Figure 1:** Thrust distributions for different values of $N_f$, using the PMC$_\infty$ (solid line) and the CSS (dashed line) [45]. The Green shaded area is the results for the values of $N_f$ taken in the conformal window. The experimental data points are taken from the ALEPH, DELPHI,OPAL, L3, SLD experiments [1–5].

A direct comparison between PMC$_\infty$ (solid line) and CSS (dashed line) is shown at different values of the number of flavors. We notice that, despite the phase transition (i.e. the transition from an infrared finite coupling to an infrared divergent coupling), the curves

given by the PMC$_\infty$ at different $N_f$, preserve with continuity the same characteristics of the conformal distribution setting $N_f$ out of the conformal window of pQCD. We notice that by decreasing $N_f$, the peak increases and this is mainly due to larger values of the $\beta_0, \beta_1$ coefficients, obtaining a better match with the data for values in the range $5 \leq N_f \leq 6$. The position of the peak of the thrust distribution is well preserved varying $N_f$ in and out of the conformal window using the PMC$_\infty$, while there is constant shift towards lower values using the CSS. These trends are shown in Fig. 2. We notice that in the central range, $2 < N_f < 15$, the position of the peak is exactly preserved using the PMC$_\infty$ and overlaps with the position of the peak shown by the experimental data. Theoretical uncertainties on the position of the peak have been calculated using standard criteria, i.e. varying the remaining initial scale value in the range $M_Z/2 \leq \mu_0 \leq 2M_Z$, and considering the lowest uncertainty given by the half of the spacing between two adjacent bins. Using the definition given in Eq. 14,

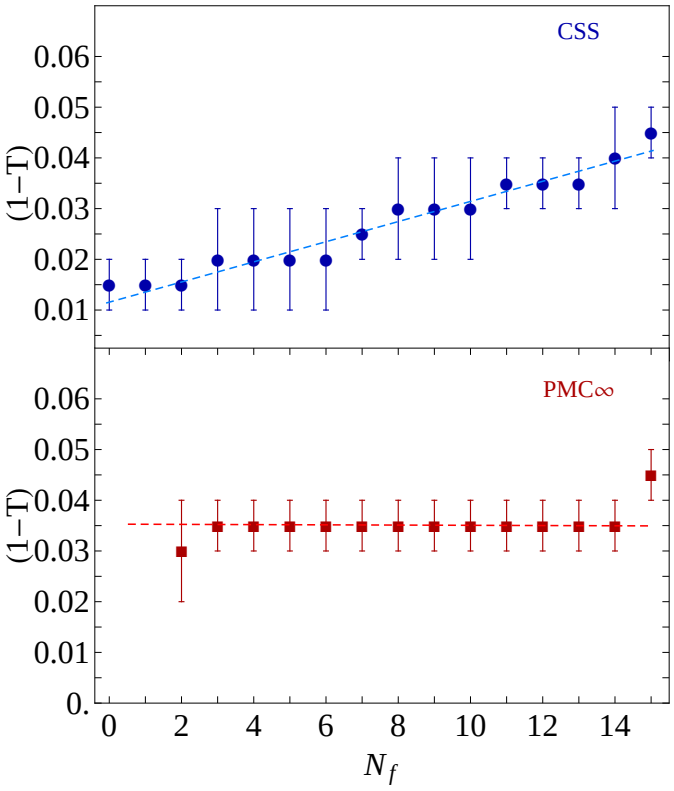


**Figure 2:** Comparison of the position of the peak for the thrust distribution using the CSS and the PMC$_\infty$ vs the number of flavors, $N_f$. Dashed lines indicate the particular trend in each graph [45].

we have determined the average error, $\bar{\delta}$, calculated in the interval $0.005 < (1-T) < 0.4$ of thrust and results for CSS and PMC$_\infty$ are shown in Fig. 3. We notice that the PMC$_\infty$ in the perturbative and IR conformal window, i.e. $12 < N_f < \bar{N}_f$, which is the region where $\alpha_s(\mu) < 1$ in the whole range of the renormalization scale values, from 0 up to $\infty$, the average error given by PMC$_\infty$ tends to zero ($\sim 0.23 - 0.26\%$) while the error given by the CSS tends to remain constant ($0.85 - 0.89\%$). The comparison of the two methods shows

that, out of the conformal window, $N_f < \frac{34N_c^3}{13N_c^2-3}$, the PMC$_\infty$ leads to a higher precision.

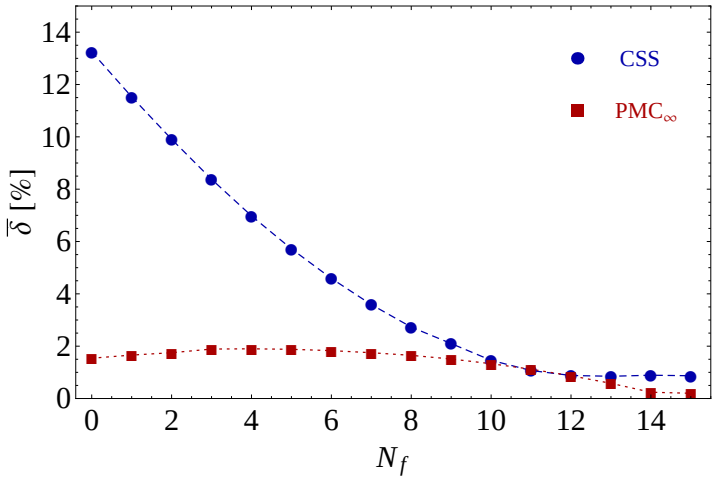


**Figure 3:** Comparison of the average theoretical error, $\bar{\delta}$, calculated using standard criteria in the range: $0.005 < (1-T) < 0.4$, using the CSS and the PMC$_\infty$ for the thrust distribution vs the number of flavors, $N_f$ [45].

## 4. The thrust distribution in the Abelian limit $N_c \to 0$

We consider now the thrust distribution in U(1) Abelian QED, which rather than being infrared interacting is infrared free. We obtain the QED thrust distribution performing the $N_c \to 0$ limit of the QCD thrust at NNLO according to [30, 61]. In the zero number of colors limit the gauge group color factors are fixed by $N_A = 1$, $C_F = 1$, $T_R = 1$, $C_A = 0$, $N_c = 0$, $N_f = N_l$, where $N_l$ is the number of active leptons, while the $\beta$-terms and the coupling rescale as $\beta_n/C_F^{n+1}$ and $\alpha_s \cdot C_F$ respectively. In particular $\beta_0 = -\frac{4}{3}N_l$ and $\beta_1 = -4N_l$ using the normalization of Eq. 1. According to this rescaling of the color factors we have determined the QED thrust and the QED PMC$_\infty$ scales. For the QED coupling, we have used the analytic formula for the effective fine structure constant in the $\overline{\rm MS}$-scheme:

$$\alpha(Q^2) = \frac{\alpha}{\left(1 - \Re e\Pi^{\overline{\rm MS}}(Q^2)\right)}, \tag{19}$$

with $\alpha^{-1} \equiv \alpha(0)^{-1} = 137.036$ and the vacuum polarization function ($\Pi$) calculated perturbatively at two loops including contributions from leptons, quarks and $W$ boson. The QED PMC$_\infty$ scales have the same form of Eqs. 17 and 18 with the factor for the $\overline{\rm MS}$-scheme set to $f_{sc} \equiv 5/6$ and the $\eta$ regularization parameter introduced to cancel singularities in the NLO PMC$_\infty$ scale $\mu_{\rm II}$ in the $N_c \to 0$ limit tends to the same QCD value, $\eta = 3.51$. A direct comparison between QED and QCD PMC$_\infty$ scales is shown in Fig. 4. We note that in the QED limit the PMC$_\infty$ scales have analogous dynamical behavior as those calculated in QCD, differences arise mainly owing to the $\overline{\rm MS}$ scheme factor reabsorption, the effects of the $N_c$ number of colors at NLO are also negligible. Thus we notice that perfect

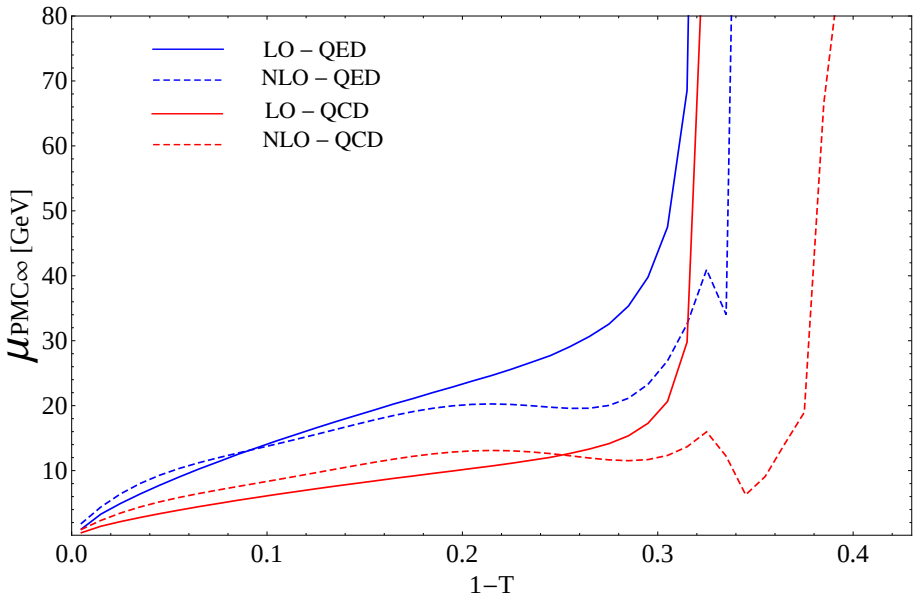


**Figure 4:** $PMC_\infty$ scales for the thrust distribution: LO-QCD scale (solid red); LO-QED scale (solid blue);NLO-QCD scale (dashed red); NLO-QED scale (dashed blue) [45].

consistency is shown from QCD to QED using the $PMC_\infty$ method. The normalized QED thrust distribution is shown in Fig. 5. We note that the curve is peaked at the origin, $T = 1$, which suggests that the three-jet event in QED occurs with a rather back-to-back symmetry. Results for the CSS and the $PMC_\infty$ methods in QED are of the order of $O(\alpha)$ and show very small differences, given the good convergence of the theory.

## 5. Conclusion

We have investigated for the first time the thrust distribution within the perturbative conformal window of QCD and in QED and we have compared results obtained using both the CSS and the $PMC_\infty$ scale setting. In the latter case the results are in perfect agreement with the Gell-Man–Low scheme. Results for different values of the $N_f$ factor show that the $PMC_\infty$ scale setting leads to higher precision and are in agreement with the data in a wide range of the selected event shape variable. Moreover the thrust distributions in the conformal window have similar shapes to those of the physical values of $N_f$ and the position of the peak is preserved when one applies the $PMC_\infty$ method. Thus, even though the peak is a property directly related to the resummation of the large-logarithms in the low-energy region [17, 62–66], the correct position of the peak can be considered in fact a conformal property and it can be related to the use of the $PMC_\infty$ scales.

## Acknowledgements

LDG thanks the organizers of RADCOR 2023 for the opportunity to give his presentation. This research was supported in part by the Department of Energy contract DE-AC02-76SF00515 (SJB). SLAC-PUB-17750.

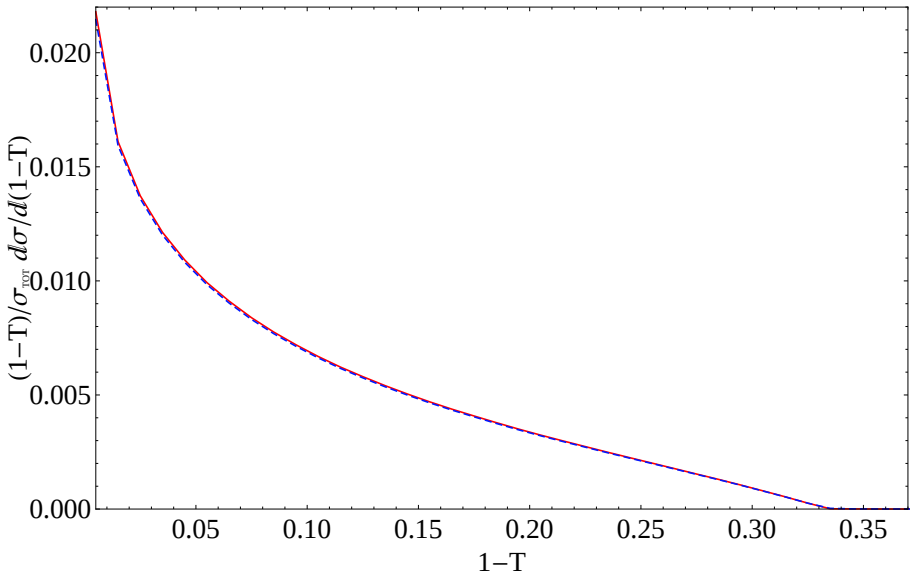


**Figure 5:** Thrust distributions in the QED limit at NNLO using the $\text{PMC}_\infty$ (solid red) and the CSS (dashed blue) [45].

## References

[1] A. Heister *et al.* [ALEPH], Eur. Phys. J. C **35**, 457-486 (2004) doi:10.1140/epjc/s2004-01891-4

[2] J. Abdallah *et al.* [DELPHI], Eur. Phys. J. C **29**, 285-312 (2003) doi:10.1140/epjc/s2003-01198-0 [arXiv:hep-ex/0307048 [hep-ex]].

[3] G. Abbiendi *et al.* [OPAL], Eur. Phys. J. C **40**, 287-316 (2005) doi:10.1140/epjc/s2005-02120-6 [arXiv:hep-ex/0503051 [hep-ex]].

[4] P. Achard *et al.* [L3], Phys. Rept. **399**, 71-174 (2004) doi:10.1016/j.physrep.2004.07.002 [arXiv:hep-ex/0406049 [hep-ex]].

[5] K. Abe *et al.* [SLD], Phys. Rev. D **51**, 962-984 (1995) doi:10.1103/PhysRevD.51.962 [arXiv:hep-ex/9501003 [hep-ex]].

[6] R. K. Ellis, D. A. Ross and A. E. Terrano, Nucl. Phys. B **178**, 421-456 (1981) doi:10.1016/0550-3213(81)90165-6

[7] Z. Kunszt, Phys. Lett. B **99**, 429-432 (1981) doi:10.1016/0370-2693(81)90563-3

[8] J. A. M. Vermaseren, K. J. F. Gaemers and S. J. Oldham, Nucl. Phys. B **187**, 301-320 (1981) doi:10.1016/0550-3213(81)90276-5

[9] K. Fabricius, I. Schmitt, G. Kramer and G. Schierholz, Z. Phys. C **11**, 315 (1981) doi:10.1007/BF01578281

[10] W. T. Giele and E. W. N. Glover, Phys. Rev. D **46**, 1980-2010 (1992) doi:10.1103/PhysRevD.46.1980

[11] S. Catani and M. H. Seymour, Phys. Lett. B **378**, 287-301 (1996) doi:10.1016/0370-2693(96)00425-X [arXiv:hep-ph/9602277 [hep-ph]].

[12] A. Gehrmann-De Ridder, T. Gehrmann, E. W. N. Glover and G. Heinrich, Comput. Phys. Commun. **185**, 3331 (2014) doi:10.1016/j.cpc.2014.07.024 [arXiv:1402.4140 [hep-ph]].

[13] A. Gehrmann-De Ridder, T. Gehrmann, E. W. N. Glover and G. Heinrich, Phys. Rev. Lett. **99**, 132002 (2007) doi:10.1103/PhysRevLett.99.132002 [arXiv:0707.1285 [hep-ph]].

[14] A. Gehrmann-De Ridder, T. Gehrmann, E. W. N. Glover and G. Heinrich, JHEP **12**, 094 (2007) doi:10.1088/1126-6708/2007/12/094 [arXiv:0711.4711 [hep-ph]].

[15] S. Weinzierl, Phys. Rev. Lett. **101**, 162001 (2008) doi:10.1103/PhysRevLett.101.162001 [arXiv:0807.3241 [hep-ph]].

[16] S. Weinzierl, JHEP **06**, 041 (2009) doi:10.1088/1126-6708/2009/06/041 [arXiv:0904.1077 [hep-ph]].

[17] R. Abbate, M. Fickinger, A. H. Hoang, V. Mateu and I. W. Stewart, Phys. Rev. D **83**, 074021 (2011) doi:10.1103/PhysRevD.83.074021 [arXiv:1006.3080 [hep-ph]].

[18] A. Banfi, H. McAslan, P. F. Monni and G. Zanderighi, JHEP **05**, 102 (2015) doi:10.1007/JHEP05(2015)102 [arXiv:1412.2126 [hep-ph]].

[19] R. L. Workman *et al.* [Particle Data Group], PTEP **2022**, 083C01 (2022) doi:10.1093/ptep/ptac097

[20] S. J. Brodsky, G. P. Lepage and P. B. Mackenzie, Phys. Rev. D **28**, 228 (1983) doi:10.1103/PhysRevD.28.228

[21] S. J. Brodsky and L. Di Giustino, Phys. Rev. D **86**, 085026 (2012) doi:10.1103/PhysRevD.86.085026 [arXiv:1107.0338 [hep-ph]].

[22] S. J. Brodsky and X. G. Wu, Phys. Rev. D **85**, 034038 (2012) [erratum: Phys. Rev. D **86**, 079903 (2012)] doi:10.1103/PhysRevD.85.034038 [arXiv:1111.6175 [hep-ph]].

[23] S. J. Brodsky and X. G. Wu, Phys. Rev. Lett. **109**, 042002 (2012) doi:10.1103/PhysRevLett.109.042002 [arXiv:1203.5312 [hep-ph]].

[24] M. Mojaza, S. J. Brodsky and X. G. Wu, Phys. Rev. Lett. **110**, 192001 (2013) doi:10.1103/PhysRevLett.110.192001 [arXiv:1212.0049 [hep-ph]].

[25] S. J. Brodsky, M. Mojaza and X. G. Wu, Phys. Rev. D **89**, 014027 (2014) doi:10.1103/PhysRevD.89.014027 [arXiv:1304.4631 [hep-ph]].

[26] S. J. Brodsky and X. G. Wu, Phys. Rev. D **86**, 054018 (2012) doi:10.1103/PhysRevD.86.054018 [arXiv:1208.0700 [hep-ph]].

[27] X. G. Wu, Y. Ma, S. Q. Wang, H. B. Fu, H. H. Ma, S. J. Brodsky and M. Mojaza, Rept. Prog. Phys. **78**, 126201 (2015) doi:10.1088/0034-4885/78/12/126201 [arXiv:1405.3196 [hep-ph]].

[28] S. Q. Wang, S. J. Brodsky, X. G. Wu, J. M. Shen and L. Di Giustino, Universe **9**, no.4, 193 (2023) doi:10.3390/universe9040193 [arXiv:2302.08153 [hep-ph]].

[29] M. Beneke, Phys. Rept. **317**, 1-142 (1999) doi:10.1016/S0370-1573(98)00130-6 [arXiv:hep-ph/9807443 [hep-ph]].

[30] S. J. Brodsky and P. Huet, Phys. Lett. B **417**, 145-153 (1998) doi:10.1016/S0370-2693(97)01209-4 [arXiv:hep-ph/9707543 [hep-ph]].

[31] R. Serber, Phys. Rev. **48**, 49 (1935) doi:10.1103/PhysRev.48.49

[32] E. A. Uehling, Phys. Rev. **48**, 55-63 (1935) doi:10.1103/PhysRev.48.55

[33] P. M. Stevenson, [arXiv:2308.05072 [hep-ph]].

[34] P. M. Stevenson, Phys. Rev. D **23**, 2916 (1981) doi:10.1103/PhysRevD.23.2916

[35] Y. Ma, X. G. Wu, H. H. Ma and H. Y. Han, Phys. Rev. D **91**, no.3, 034006 (2015) doi:10.1103/PhysRevD.91.034006 [arXiv:1412.8514 [hep-ph]].

[36] Y. Ma and X. G. Wu, Phys. Rev. D **97**, no.3, 036024 (2018) doi:10.1103/PhysRevD.97.036024 [arXiv:1707.09886 [hep-ph]].

[37] X. G. Wu, J. M. Shen, B. L. Du and S. J. Brodsky, Phys. Rev. D **97**, no.9, 094030 (2018) doi:10.1103/PhysRevD.97.094030 [arXiv:1802.09154 [hep-ph]].

[38] X. G. Wu, J. M. Shen, B. L. Du, X. D. Huang, S. Q. Wang and S. J. Brodsky, Prog. Part. Nucl. Phys. **108**, 103706 (2019) doi:10.1016/j.ppnp.2019.05.003 [arXiv:1903.12177 [hep-ph]].

[39] L. Di Giustino, S. J. Brodsky, P. G. Ratcliffe, X. G. Wu and S. Q. Wang, [arXiv:2307.03951 [hep-ph]].

[40] L. Di Giustino, [arXiv:2205.03689 [hep-ph]].

[41] X. D. Huang, J. Yan, H. H. Ma, L. Di Giustino, J. M. Shen, X. G. Wu and S. J. Brodsky, Nucl. Phys. B **989**, 116150 (2023) doi:10.1016/j.nuclphysb.2023.116150 [arXiv:2109.12356 [hep-ph]].

[42] S. Q. Wang, S. J. Brodsky, X. G. Wu, L. Di Giustino and J. M. Shen, Phys. Rev. D **102**, no.1, 014005 (2020) doi:10.1103/PhysRevD.102.014005 [arXiv:2002.10993 [hep-ph]].

[43] S. Q. Wang, C. Q. Luo, X. G. Wu, J. M. Shen and L. Di Giustino, JHEP **09**, 137 (2022) doi:10.1007/JHEP09(2022)137 [arXiv:2112.06212 [hep-ph]].

[44] L. Di Giustino, S. J. Brodsky, S. Q. Wang and X. G. Wu, Phys. Rev. D **102**, no.1, 014015 (2020) doi:10.1103/PhysRevD.102.014015 [arXiv:2002.01789 [hep-ph]].

[45] L. Di Giustino, F. Sannino, S. Q. Wang and X. G. Wu, Phys. Lett. B **823**, 136728 (2021) doi:10.1016/j.physletb.2021.136728 [arXiv:2104.12132 [hep-ph]].

[46] S. Q. Wang, S. J. Brodsky, X. G. Wu and L. Di Giustino, Phys. Rev. D **99**, no.11, 114020 (2019) doi:10.1103/PhysRevD.99.114020 [arXiv:1902.01984 [hep-ph]].

[47] S. Q. Wang, S. J. Brodsky, X. G. Wu, J. M. Shen and L. Di Giustino, Phys. Rev. D **100**, no.9, 094010 (2019) doi:10.1103/PhysRevD.100.094010 [arXiv:1908.00060 [hep-ph]].

[48] D. J. Gross and F. Wilczek, Phys. Rev. Lett. **30**, 1343-1346 (1973) doi:10.1103/PhysRevLett.30.1343

[49] H. D. Politzer, Phys. Rev. Lett. **30**, 1346-1349 (1973) doi:10.1103/PhysRevLett.30.1346

[50] W. E. Caswell, Phys. Rev. Lett. **33**, 244 (1974) doi:10.1103/PhysRevLett.33.244

[51] D. R. T. Jones, Nucl. Phys. B **75**, 531 (1974) doi:10.1016/0550-3213(74)90093-5

[52] E. Egorian and O. V. Tarasov, Teor. Mat. Fiz. **41**, 26-32 (1979) JINR-E2-11757.

[53] M. Mojaza, C. Pica and F. Sannino, Phys. Rev. D **82**, 116009 (2010) doi:10.1103/PhysRevD.82.116009 [arXiv:1010.4798 [hep-ph]].

[54] T. Banks and A. Zaks, Nucl. Phys. B **196**, 189-204 (1982) doi:10.1016/0550-3213(82)90035-9

[55] E. Gardi, G. Grunberg and M. Karliner, JHEP **07**, 007 (1998) doi:10.1088/1126-6708/1998/07/007 [arXiv:hep-ph/9806462 [hep-ph]].

[56] T. A. Ryttov and R. Shrock, Phys. Rev. D **96**, no.10, 105018 (2017) doi:10.1103/PhysRevD.96.105018 [arXiv:1706.06422 [hep-th]].

[57] S. J. Brodsky, G. F. de Teramond and A. Deur, Phys. Rev. D **81**, 096010 (2010) doi:10.1103/PhysRevD.81.096010 [arXiv:1002.3948 [hep-ph]].

[58] S. Kluth, Rept. Prog. Phys. **69**, 1771-1846 (2006) doi:10.1088/0034-4885/69/6/R04 [arXiv:hep-ex/0603011 [hep-ex]].

[59] V. Del Duca, C. Duhr, A. Kardos, G. Somogyi, Z. Szőr, Z. Trócsányi and Z. Tulipánt, Phys. Rev. D **94**, no.7, 074019 (2016) doi:10.1103/PhysRevD.94.074019 [arXiv:1606.03453 [hep-ph]].

[60] V. Del Duca, C. Duhr, A. Kardos, G. Somogyi and Z. Trócsányi, Phys. Rev. Lett. **117**, no.15, 152004 (2016) doi:10.1103/PhysRevLett.117.152004 [arXiv:1603.08927 [hep-ph]].

[61] A. L. Kataev and V. S. Molokoedov, Phys. Rev. D **92**, no.5, 054008 (2015) doi:10.1103/PhysRevD.92.054008 [arXiv:1507.03547 [hep-ph]].

[62] S. Catani, G. Turnock, B. R. Webber and L. Trentadue, Phys. Lett. B **263**, 491-497 (1991) doi:10.1016/0370-2693(91)90494-B

[63] S. Catani, L. Trentadue, G. Turnock and B. R. Webber, Nucl. Phys. B **407**, 3-42 (1993) doi:10.1016/0550-3213(93)90271-P

[64] S. Catani, M. L. Mangano, P. Nason and L. Trentadue, Nucl. Phys. B **478**, 273-310 (1996) doi:10.1016/0550-3213(96)00399-9 [arXiv:hep-ph/9604351 [hep-ph]].

[65] U. Aglietti, L. Di Giustino, G. Ferrera and L. Trentadue, Phys. Lett. B **651**, 275-292 (2007) doi:10.1016/j.physletb.2007.06.034 [arXiv:hep-ph/0612073 [hep-ph]].

[66] U. Aglietti, L. Di Giustino, G. Ferrera, A. Renzaglia, G. Ricciardi and L. Trentadue, Phys. Lett. B **653**, 38-52 (2007) doi:10.1016/j.physletb.2007.07.041 [arXiv:0707.2010 [hep-ph]].